
A COMPACT, PI-MODE EXTRACTION SCHEME FOR THE AXIAL B-FIELD RECIRCULATING PLANAR MAGNETRON

Brad W. Hoff, et al.

23 July 2012

() Report

APPROVED FOR PUBLIC RELEASE; DISTRIBUTION IS UNLIMITED.



AIR FORCE RESEARCH LABORATORY
Directed Energy Directorate
3550 Aberdeen Ave SE
AIR FORCE MATERIEL COMMAND
KIRTLAND AIR FORCE BASE, NM 87117-5776

NOTICE AND SIGNATURE PAGE

Using Government drawings, specifications, or other data included in this document for any purpose other than Government procurement does not in any way obligate the U.S. Government. The fact that the Government formulated or supplied the drawings, specifications, or other data does not license the holder or any other person or corporation; or convey any rights or permission to manufacture, use, or sell any patented invention that may relate to them.

This report was cleared for public release by the Air Force Research Laboratory [insert TD site] Public Affairs Office and is available to the general public, including foreign nationals. Copies may be obtained from the Defense Technical Information Center (DTIC) (<http://www.dtic.mil>).

AFRL-RD-PS-TR-2012-0039 HAS BEEN REVIEWED AND IS APPROVED FOR PUBLICATION IN ACCORDANCE WITH ASSIGNED DISTRIBUTION STATEMENT.

//Signed//
BRAD W. HOFF, DR-II
Project Officer

//Signed//
STEPHEN T. MARTINICK, DR-IV
Chief, High Power Microwave Divison

This report is published in the interest of scientific and technical information exchange, and its publication does not constitute the Government's approval or disapproval of its ideas or findings.

REPORT DOCUMENTATION PAGE

Form Approved
OMB No. 0704-0188

Public reporting burden for this collection of information is estimated to average 1 hour per response, including the time for reviewing instructions, searching existing data sources, gathering and maintaining the data needed, and completing and reviewing this collection of information. Send comments regarding this burden estimate or any other aspect of this collection of information, including suggestions for reducing this burden to Department of Defense, Washington Headquarters Services, Directorate for Information Operations and Reports (0704-0188), 1215 Jefferson Davis Highway, Suite 1204, Arlington, VA 22202-4302. Respondents should be aware that notwithstanding any other provision of law, no person shall be subject to any penalty for failing to comply with a collection of information if it does not display a currently valid OMB control number. **PLEASE DO NOT RETURN YOUR FORM TO THE ABOVE ADDRESS.**

1. REPORT DATE (DD-MM-YYYY) 23-07-2012		2. REPORT TYPE Technical Report		3. DATES COVERED (From - To) Aug 2011 – July 2012	
4. TITLE AND SUBTITLE A Compact, Pi-Mode Extraction Scheme for the Axial B-Field Recirculating Planar Magnetron				5a. CONTRACT NUMBER In-House	
				5b. GRANT NUMBER	
				5c. PROGRAM ELEMENT NUMBER	
6. AUTHOR(S) B. W. Hoff, M. Franzi, D.M. French, G. Greening, R.M Gilgenbach				5d. PROJECT NUMBER	
				5e. TASK NUMBER D00E	
				5f. WORK UNIT NUMBER PPM00000974 DF702172	
7. PERFORMING ORGANIZATION NAME(S) AND ADDRESS(ES) Air Force Research Laboratory 3550 Aberdeen Avenue SE Kirtland AFB, NM 87117-5776				8. PERFORMING ORGANIZATION REPORT NUMBER	
9. SPONSORING / MONITORING AGENCY NAME(S) AND ADDRESS(ES) Air Force Research Laboratory 3550 Aberdeen Avenue SE Kirtland AFB, NM 87117-5776				10. SPONSOR/MONITOR'S ACRONYM(S) AFRL/RDHP	
				11. SPONSOR/MONITOR'S REPORT NUMBER(S) AFRL-RD-PS-TR-2012-0039	
12. DISTRIBUTION / AVAILABILITY STATEMENT Approved for public release; distribution is unlimited.					
13. SUPPLEMENTARY NOTES Approved for public release; 377 ABW-2012-1198 Government Purpose Rights					
14. ABSTRACT A recirculating planar magnetron (RPM), operating in the π -mode and utilizing a compact, waveguide-based extraction scheme was simulated using ICEPIC. At an applied voltage of 300 kV and B-field of 0.140T, output power of the six-module RPM was 565 MW with 33% efficiency. The oscillator was found to operate at frequency of 2.245 GHz. Increasing the number of extracted modules in the RPM was found to result a linear increase in power at the rate of 120 MW per module.					
15. SUBJECT TERMS Recirculating Planar Magnetron; RF Extraction; HPM					
16. SECURITY CLASSIFICATION OF:			17. LIMITATION OF ABSTRACT SAR	18. NUMBER OF PAGES 20	19a. NAME OF RESPONSIBLE PERSON Brad W. Hoff
a. REPORT UNCLASS	b. ABSTRACT UNCLASS	c. THIS PAGE UNCLASS			19b. TELEPHONE NUMBER (include area code)

Standard Form 298 (Rev. 8-98)
Prescribed by ANSI Std. Z39.18

This page intentionally left blank.

Table of Contents

Table of Figures.....	iv
Abstract.....	v
Keywords.....	v
1.0 Introduction	1
2.0 Waveguide Design.....	2
3.0 RPM Simulations	4
4.0 Simulation Analysis	9
Acknowledgements.....	10
References	11

Table of Figures

Figure 1. Axial B-field RPM, without extraction, as described in Refs. [1], [2].	1
Figure 2. A compact, all cavity extraction technique for cylindrical magnetrons, as described in Refs. [3], [4].	1
Figure 3. Maximum theoretical efficiencies calculated using equation (3) for magnetron phase velocities of $0.24c$, $0.34c$, and $0.5c$.	3
Figure 4. Electric field distribution for a ridged waveguide proposed for use in RF extraction of a RPM with a center frequency around 2.25 GHz.	3
Figure 5. (a) Calculated S_{21} for a one meter section of the ridged waveguide described in Figure 4 and (b) calculated peak electric field within the waveguide compared with the Kilpatrick Limit of 41 MV/m at 2.25 GHz.	4
Figure 6. Cross sectional geometry of the simulated RPM parallel to the (a) X-Y plane and (b) X-Z plane. The following numbered components are depicted: 1. cathode, 2. anode vane, 3. anode cavity, 4. waveguide, 5. waveguide ridges, 6. an RPM module, 7. aperture, 8. cathode electrostatic end caps, 9. waveguide load (perfectly matched layer (PML) [13]), 10. voltage wave injection port.	5
Figure 7. Detailed simulation geometry of the extracted RPM simulation. Measurements are in centimeters. Extraction apertures are four centimeters in length.	5
Figure 8. (a) Power, voltage, current, and efficiency data and (b) frequency data for a 6-module extracted RPM operating with an axial magnetic field of 0.14 T.	6
Figure 9. Particle plots of the operating 6-module RPM: X-Y plane (a) and X-Z plane (b).	7
Figure 10. (a) Upper and lower waveguide power for each RPM module along with (b) module designation and $E \times B$ direction.	8
Figure 11. Power and efficiency as a function of total number of modules for various extracted RPMs.	9
Figure 12. Inter-vane voltage data for the leftmost cavity of each of the six voltage modules of the upper RPM section.	10

Abstract

A recirculating planar magnetron (RPM), operating in the π -mode and utilizing a compact, waveguide-based extraction scheme was simulated using ICEPIC. At an applied voltage of 300 kV and B-field of 0.140T, output power of the six-module RPM was 565 MW with 33% efficiency. The oscillator was found to operate at frequency of 2.245 GHz. Increasing the number of extracted modules in the RPM was found to result a linear increase in power at the rate of 120 MW per module.

Keywords:

Recirculating Planar Magnetron; RF Extraction; HPM

This page intentionally left blank.

1.0 Introduction

Recent work by Gilgenbach, et al., describes a new class of magnetron, namely, the recirculating planar magnetron (RPM) [1], [2]. These crossed-field oscillators have a number of potential advantages, including rapid start-up, reduced cathode loading, and enhanced heat dissipation, when compared to standard cylindrical magnetron geometries. One of the variants of the RPM concept described by Ref [1] and Ref [2] is the axial B-field RPM. An example of this type of RPM is shown in Figure 1.

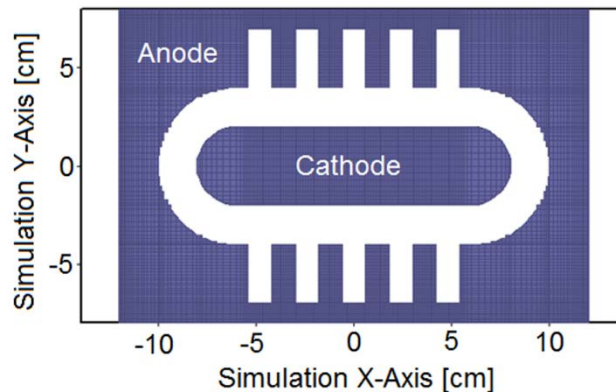


Figure 1. Axial B-field RPM, without extraction, as described in Refs. [1], [2].

The work described here involves using ICEPIC to computationally model the incorporation of a compact, axial, waveguide-based extraction scheme into the axial B-field variant of the RPM described in Refs. [1] and [2]. This extraction scheme, as presented by Greenwood in [3] and in follow-on work by Hoff et al. [4], magnetically couples microwave energy from two neighboring cavities of a cylindrical magnetron operating in the π -mode into an adjacent waveguide exciting a TE₁₀-like mode. Figure 2 depicts a cross section of a magnetron using the extraction concept described in [3].

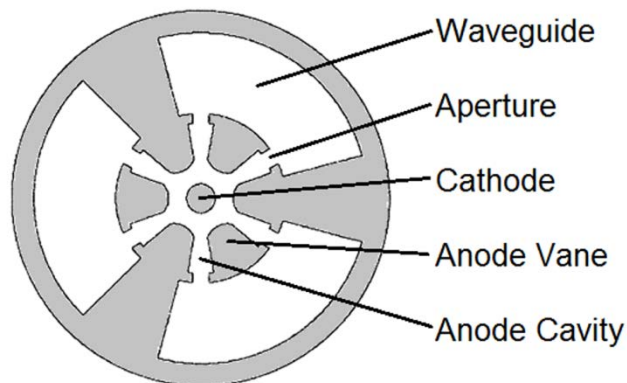


Figure 2. A compact, all cavity extraction technique for cylindrical magnetrons, as described in Refs. [3], [4].

2.0 Waveguide Design

Because of the requirement of two adjacent cavities coupling into a single waveguide, Greenwood's extraction concept [3] imposes certain additional constraints on magnetron design. In standard rectangular waveguide, the longest cross sectional dimension, which we will call d_a determines the cutoff frequency, f_c , for the lowest order guided mode (TE₁₀), as shown in equation (1):

$$f_c = \frac{c}{2d_a} \quad (1)$$

In equation (1), c is the speed of light. The π mode wavelength, λ_π , in slow wave structures such as that common to magnetrons [5] is equal to the distance across two vanes and two cavities, which, in this case, must equal to d_a (the waveguide cross sectional dimension parallel to the Y Axis in Figure 4). Thus, in a planar magnetron, the minimum phase velocity, v_{ph} , to stay above cutoff in the rectangular waveguide is

$$v_{ph} = f_c \lambda_\pi = \frac{c}{2d_a} d_a = \frac{c}{2}. \quad (2)$$

In most electron beam driven microwave sources, such as magnetrons, electrons must be accelerated such that they are in synchronism with the phase velocity, v_{ph} , of the electromagnetic wave for an energy exchange with the electromagnetic wave to take place. In order for an electron in a magnetron to reach this velocity, a certain portion of the electric potential energy that exists as the applied voltage across the A-K gap, must be converted to kinetic energy as the electron moves from the cathode towards the anode. The remainder of the potential energy is available to be contributed to the electromagnetic wave. The fraction of the remaining potential energy divided by the total applied gap potential can be thought of as a measure of the maximum theoretical efficiency, given by

$$Eff_{max} = 1 - \frac{KE}{PE} = 1 - \frac{(\gamma-1)mc^2}{eV}, \quad (3)$$

where $\gamma = (1 - v_{ph}^2/c^2)^{-1/2}$ and v_{ph} is the π mode phase velocity.

A plot of the maximum theoretical efficiency for magnetron operation with $v_{ph} = 0.5c$ as a function of applied voltage is given in Figure 3. Also shown in Figure 3 are the maximum theoretical efficiency plots for phase velocities of $0.24c$ and $0.34c$, which are bounding values for the π mode phase velocities of a number of relativistic magnetrons found in published literature [6], [7]. The operating voltage chosen for the present RPM simulations, 300 kV, is also indicated in Figure 3.

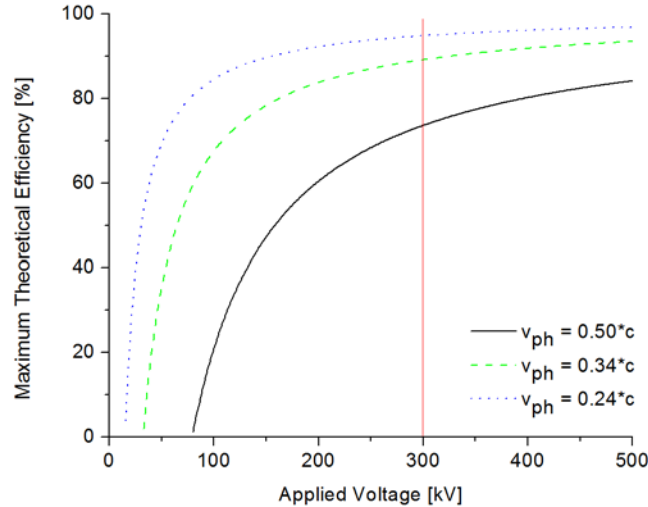


Figure 3. Maximum theoretical efficiencies calculated using equation (3) for magnetron phase velocities of 0.24c, 0.34c, and 0.5c.

One method to reduce the overall waveguide cross sectional dimensions while maintaining the bandwidth necessary to extract microwave energy from the magnetron is by including capacitive ridges within the waveguide [8]. Figure 4 depicts cross sectional geometry of the extraction waveguides chosen for use with the RPM. Overlaid with the waveguide geometry is a contour plot of the calculated electric field magnitude for the lowest order waveguide mode at the RPM design frequency, 2.25 GHz. As would be expected, and is shown in Figure 4, the highest electric field stresses occur between the two capacitive waveguide ridges.

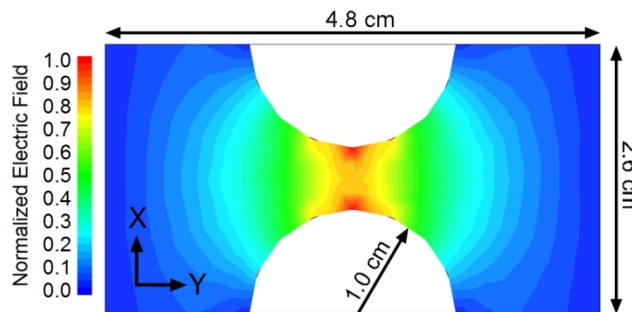


Figure 4. Electric field distribution for a ridged waveguide proposed for use in RF extraction of a RPM with a center frequency around 2.25 GHz.

Using the Ansys HFSS software suite [9], calculations were performed to determine two port network parameters for a one meter length of the ridged waveguide. A plot of ridged waveguide S_{21} magnitude as a function of frequency is displayed in Figure 5 (a). Waveguide cutoff was found to occur at approximately 2.0 GHz, providing ample frequency margin for operation of the RPM at the 2.25 GHz design frequency.

Because of the enhanced electric field magnitude due to the presence of the waveguide ridges, additional calculations were performed to determine proximity to the Kilpatrick limit [10]; the results of which are displayed in Figure 5 (b). It is important to note that the Kilpatrick

limit is provided only as a reference point, as proper surface conditioning routinely allows operation at many times the Kilpatrick limit [11].

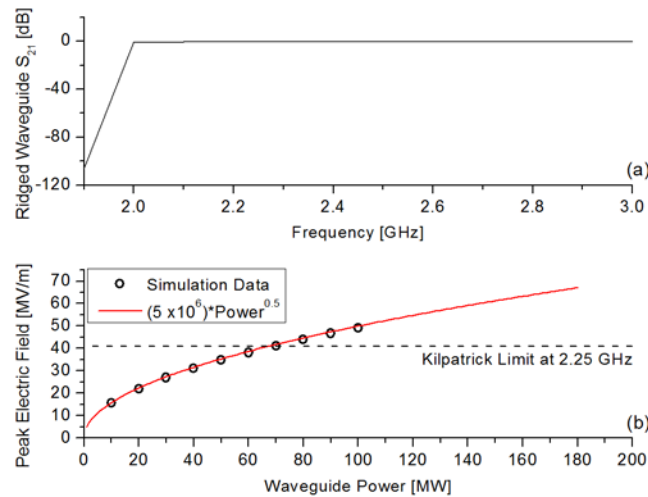


Figure 5. (a) Calculated S21 for a one meter section of the ridged waveguide described in Figure 4 and (b) calculated peak electric field within the waveguide compared with the Kilpatrick Limit of 41 MV/m at 2.25 GHz.

With a waveguide width of 4.8 cm, as shown in Figure 4, and an assumed waveguide wall thickness of 2 cm, the total distance spanned by one full π mode spatial wavelength will be 5.2 cm. At the design frequency of 2.25 GHz, the π mode phase velocity is equal to $0.39 \cdot c$. Thus the calculated maximum theoretical efficiency at the RPM design frequency is 85.4%.

3.0 RPM Simulations

The particle-in-cell code ICEPIC [12] was used to simulate the extracted recirculating planar magnetron. Figure 6 depicts cross sectional geometry of the simulated RPM, with metal shown in grey and the interior vacuum region shown in white. A cross section parallel to the X-Y plane which bisects the anode block is given in Figure 6 (a) and a cross section parallel to the X-Z plane is given in Figure 6 (b). A Cartesian grid was used with resolution equal to 1 mm in all three axes. The cathode section between the two electrostatic end caps was allowed to emit using ICEPIC's explosive emission model with the emission threshold set to 2 MV/m. Further details on the slow wave structure geometry are provided in Figure 7.

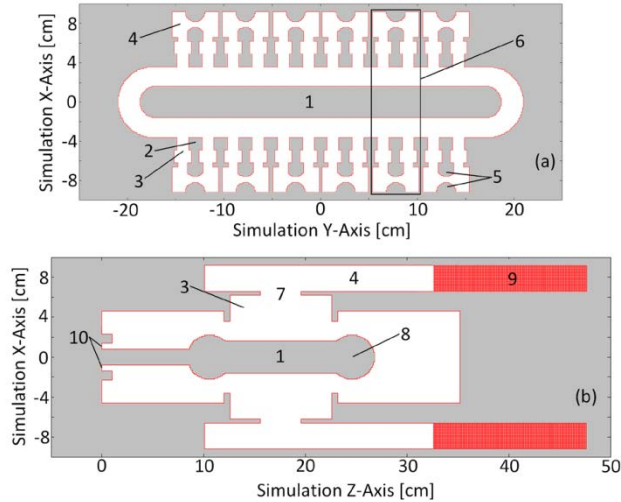


Figure 6. Cross sectional geometry of the simulated RPM parallel to the (a) X-Y plane and (b) X-Z plane. The following numbered components are depicted: 1. cathode, 2. anode vane, 3. anode cavity, 4. waveguide, 5. waveguide ridges, 6. an RPM module, 7. aperture, 8. cathode electrostatic end caps, 9. waveguide load (perfectly matched layer (PML) [13]), 10. voltage wave injection port.

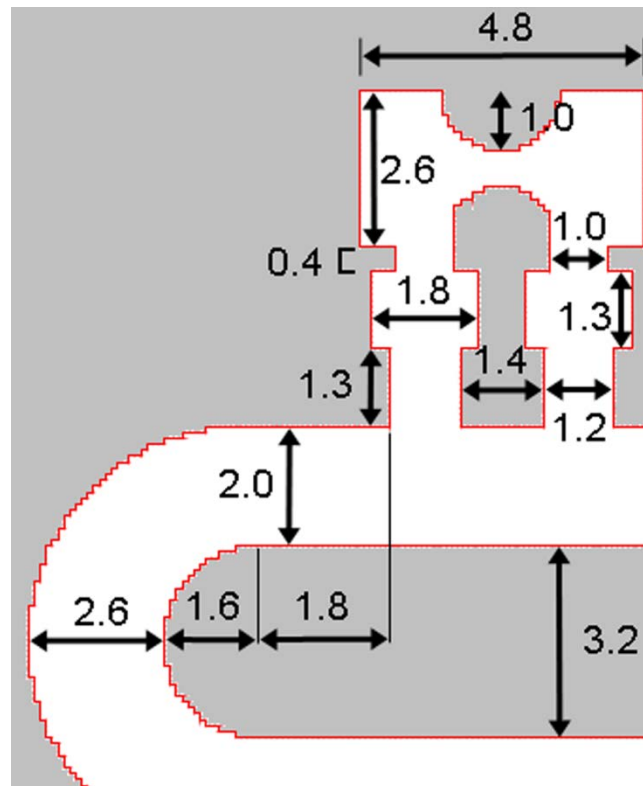


Figure 7. Detailed simulation geometry of the extracted RPM simulation. Measurements are in centimeters. Extraction apertures are four centimeters in length.

Because the MELBA-C accelerator was identified as a likely test-bed for follow-on extracted RPM experiments, the operating voltage for the RPM simulations was selected to be around 300 kV, approximating operating voltage values described in previous magnetron work [7], [14]. In order to select a magnetic field for RPM operation, an initial estimation was made, based on the usual relativistic Buneman-Hartree relationship [15], equation 5, in conjunction with the approximately 2.25 GHz π mode cold frequency. The magnetic field was then iterated in the simulation hot tests until optimal π mode oscillation was observed.

Figure 8 depicts data obtained in simulated hot tests using the 6-module RPM simulation geometry of Figure 6 operating with a 0.14 T axial magnetic field. As previously stated, for the purposes of this discussion, an RPM “module” is a pairing of an upper and lower extraction waveguide and associated vanes, cavities and cathode area. Steady state power and efficiency values were 565 MW and 33%, respectively, as shown in Figure 8 (a). Operating impedance was approximately 46 Ohms. Data from a FFT of inter-vane voltage measurements are plotted in Figure 8 (b). The operating spectrum showed no evidence of mode competition, with a center frequency of 2.245 GHz. Particle plots for the simulated RPM in planes parallel to the X-Y plane and X-Z plane are presented in Figure 9 (a) and Figure 9 (b), respectively.

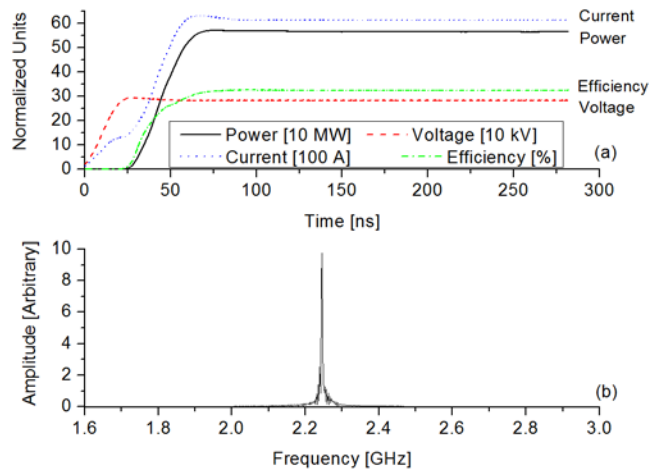


Figure 8. (a) Power, voltage, current, and efficiency data and (b) frequency data for a 6-module extracted RPM operating with an axial magnetic field of 0.14 T.

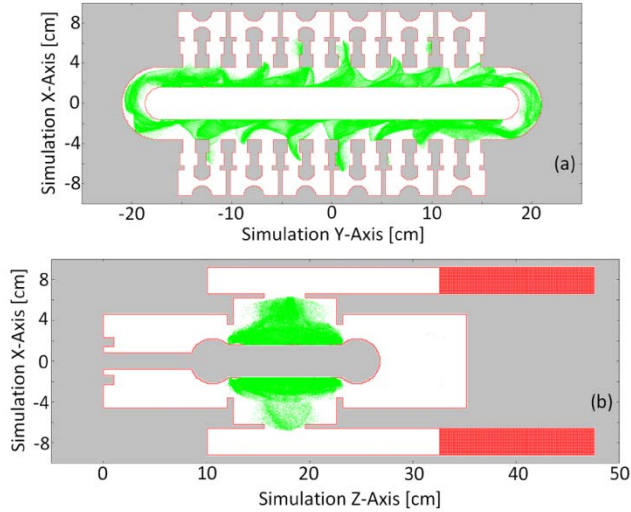


Figure 9. Particle plots of the operating 6-module RPM: X-Y plane (a) and X-Z plane (b).

Waveguide power for each of the extraction waveguides was sampled during steady state operation and is plotted in Figure 10 (a). As would be expected from an inspection of relative spoke height in each of the RPM modules along the length of the device, extracted power in each waveguide is maximum in the center waveguides then tapers off toward the end modules. Interestingly, when the power of each waveguide is compared in conjunction with the $E \times B$ drift direction (i.e. comparing modules in the order one to six in the upper section and in the order six to one in the lower section, as shown in Figure 10 (b)), the power variation profile of the upper and lower sections is almost identical. The 70 MW power loading for the module three and four waveguides are predicted to have peak electric fields on the waveguide ridges at close to the Kilpatrick Limit at 2.25 GHz, as calculated for Figure 5.

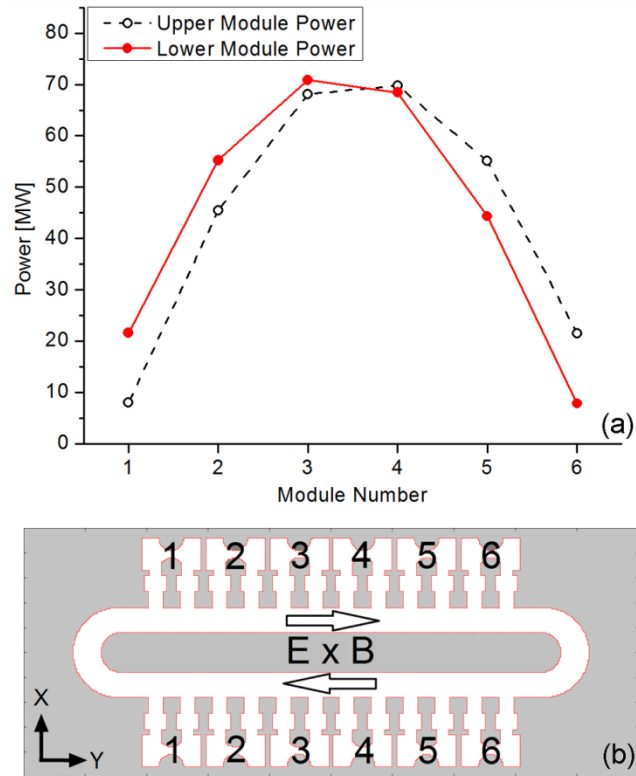


Figure 10. (a) Upper and lower waveguide power for each RPM module along with (b) module designation and $E \times B$ direction.

In order to study power scaling in the present extracted RPM concept, RPMs with various numbers of modules, ranging from one to 16, were simulated and compared. The data from this series of simulations are plotted in Figure 11. The RPMs with only one or two modules were found to exhibit unstable operation, if oscillation occurred at all. For modules with three or more modules, total output power was found to scale linearly, at a rate of 120 MW per module. Operating efficiency for the stable RPMs was found to remain around 33%.

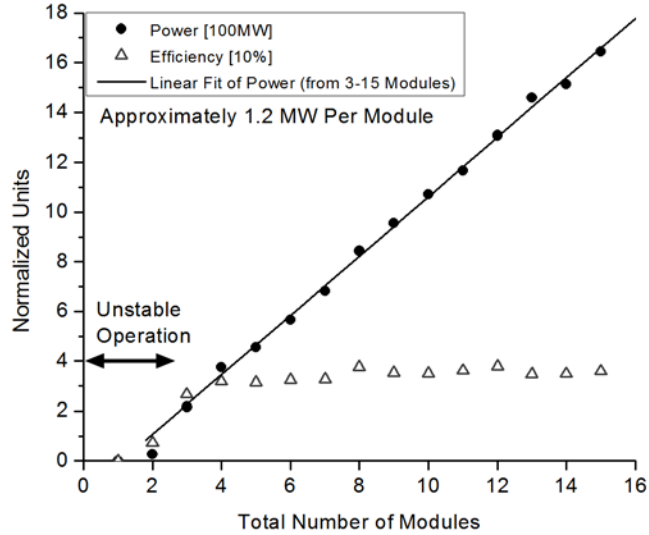


Figure 11. Power and efficiency as a function of total number of modules for various extracted RPMs.

4.0 Simulation Analysis

While the simulated 6-module RPM in this study was found to show no evidence of mode competition in the hot test frequency spectrum, shown in Figure 8 (b), careful examination of the particle data in Figure 9 (a) and (b) show a phase shift from module to module that is uncharacteristic of true π -mode operation. In π mode operation, the phase shift from the beginning of one module to the beginning of the next adjacent one should be zero (because the phase shift between adjacent cavities should be π radians). Figure 12 depicts time dependent inter-vane voltage measurements for the leftmost cavity of each module of the top RPM section. These data are taken during two separate time periods: 99.0 ns to 100.0 ns in Figure 12 (a) and 207.7 ns to 208.7 ns in Figure 12 (b). The relative phase change of the RF wave between each of the module sections was found to remain constant for the duration of steady-state operation of the RPM.

The source of this additional phase shift between modules may be a result of the choice of recirculating sections connecting the upper and lower linear magnetron sections. The recirculating end-section geometry was chosen based on early 2-D simulations of RPMs without extraction and was not optimized in any way as part of this study. The phase mismatch created by the recirculating end-sections shifts over the spatial extent of the linear magnetron sections via nonlinear interactions with the beam. This behavior is also likely to be a factor in the waveguide power-loading profile data displayed in Figure 10 (a). It is expected that a careful optimization of the recirculating end-sections of the RPM would correct the inter-module phase shifts, as well as balance power across the waveguides in the upper and lower magnetron sections, and potentially favorably affecting operating efficiency.

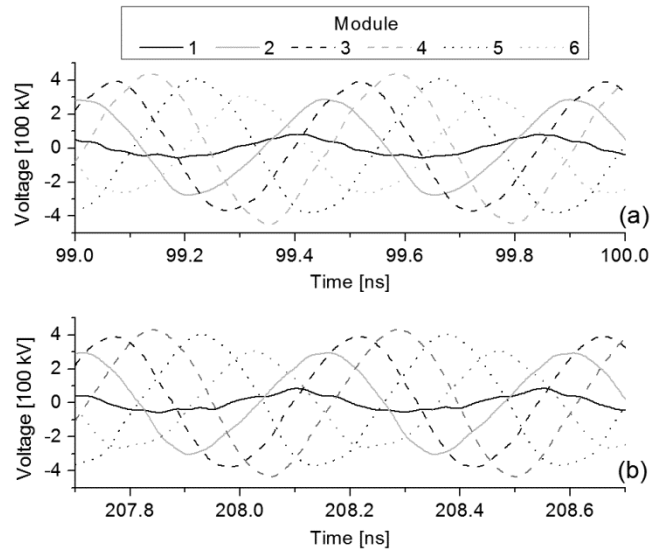


Figure 12. Inter-vane voltage data for the leftmost cavity of each of the six voltage modules of the upper RPM section.

Acknowledgements

This effort was supported by the Air Force Office of Scientific Research under AFOSR LRIR 11RD01COR and by the Department of Defense High Performance Computer Modernization Program under subproject AFKED01314C4O. The authors would like to acknowledge helpful discussions with A. D. Greenwood and P. J. Mardahl of the Air Force Research Laboratory regarding the ICEPIC code.

References

- [1] R. M. Gilgenbach, Y.-Y. Lau, D. M. French, B. W. Hoff, J. Luginsland, and M. Franzi, "Crossed Field Device," U.S. Patent Filing 12/860,336.
- [2] R. M. Gilgenbach, Yue-Ying Lau, D. M. French, B. W. Hoff, M. Franzi, and J. Luginsland, "Recirculating Planar Magnetrons for High-Power High-Frequency Radiation Generation," *IEEE Trans Plasma Sci.*, vol. 39, no. 4, pp. 980–987, Apr. 2011.
- [3] A. D. Greenwood, "All cavity magnetron axial extractor," U.S. Patent 710600412-Sep-2006.
- [4] B. W. Hoff, A. D. Greenwood, P. J. Mardahl, and M. D. Haworth, "All Cavity Magnetron Axial Extraction Technique," *IEEE Trans. Plasma Sci.*, no. (Submitted April 2012).
- [5] G. B. Collins, Ed., *Microwave Magnetrons*, 1st ed., vol. 6. New York: McGraw-Hill, 1948.
- [6] A. Palevsky and G. Bekefi, "Microwave emission from pulsed, relativistic e-beam diodes. II. The multiresonator magnetron," *Physics of Fluids*, vol. 22, no. 5, p. 986, May 1979.
- [7] M. R. Lopez, R. M. Gilgenbach, M. C. Jones, W. M. White, D. W. Jordan, M. D. Johnston, T. S. Strickler, V. B. Neculaes, Y. Y. Lau, T. A. Spencer, M. D. Haworth, K. L. Cartwright, P. J. Mardahl, J. W. Luginsland, and D. Price, "Relativistic magnetron driven by a microsecond E-beam accelerator with a ceramic insulator," *IEEE Trans. Plasma Sci.*, vol. 32, no. 3, pp. 1171–1180, 2004.
- [8] H. P. Westman, *Reference Data for Radio Engineers*, 5th ed. Howard W. Sams & Co., Inc., 1982.
- [9] "<http://www.ansoft.com/products/hf/hfss/>."
- [10] W. D. Kilpatrick, "Criterion for Vacuum Sparking Designed to Include Both rf and dc," *Rev. Sci. Instrum.*, vol. 28, no. 10, pp. 824–826, Oct. 1957.
- [11] E. Tanabe, J. W. Wang, and G. A. Loew, "Voltage Breakdown at X-band and C-band Frequencies," in *Proceedings of the 1986 Linear Accelerator Conference*, Stanford, CA, 1986.
- [12] R. E. Peterkin and J. W. Luginsland, "A Virtual Prototyping Environment for Directed-Energy Concepts," *Comput. Sci. Eng.*, vol. 4, no. 2, pp. 42–49, Mar. 2002.
- [13] B. Jean-Pierre, "A perfectly matched layer for the absorption of electromagnetic waves," *J. Comput. Phys.*, vol. 114, no. 2, pp. 185–200, Oct. 1994.
- [14] M. R. Lopez, R. M. Gilgenbach, D. W. Jordan, S. A. Anderson, M. D. Johnston, M. W. Keyser, H. Miyake, C. W. Peters, M. C. Jones, V. Bogdan Neculaes, Y. Y. Lau, T. A. Spencer, J. W. Luginsland, M. D. Haworth, R. W. Lemke, and D. Price, "Cathode effects on a relativistic magnetron driven by a microsecond e-beam accelerator," *Plasma Science, IEEE Transactions on*, vol. 30, no. 3, pp. 947 – 955, Jun. 2002.
- [15] R. V. Lovelace and T. F. T. Young, "Relativistic Hartree condition for magnetrons: Theory and comparison with experiments," *Phys. Fluids*, vol. 28, no. 8, pp. 2450–2452, 1985.

DISTRIBUTION LIST

DTIC/OCP 8725 John J. Kingman Rd, Suite 0944 Ft Belvoir, VA 22060-6218	1 cy
AFRL/RVIL Kirtland AFB, NM 87117-5776	1 cy
Official Record Copy AFRL/RDHP/Brad Hoff	1 cy